Hindawi
Wireless Communications and Mobile Computing
Volume 2022, Article ID 3892542, 15 pages
https://doi.org/10.1155/2022/3892542

Research Article

Simple Direction-of-Arrival Estimation under Nonuniform Noise Scenarios

Fenggang Sun,[1] Jiefang Wu,[2] Hao Fan,[1] Lizhen Chen,[1] and Peng Lan[1]

[1]*College of Information Science and Engineering, Shandong Agricultural University, Tai'an 271018, China*
[2]*School of Mathematics and Statistics, Taishan University, Tai'an 271018, China*

Correspondence should be addressed to Peng Lan; lanpeng@sdau.edu.cn

Received 5 April 2022; Revised 27 April 2022; Accepted 9 May 2022; Published 26 May 2022

Academic Editor: Jian Feng Li

The uniform white noise assumption is widely applied for most of the existing direction-of-arrival (DOA) estimation methods, which however may degrade the estimation performance. In practical scenarios, the nonuniform white noise model is more adequate. In this paper, we propose a simple DOA estimation method in the presence of spatially nonuniform white noise with unknown noise covariance matrix. The estimate of the unknown noise covariance matrix is firstly obtained by utilizing the shift property of identical subarrays. Then, the received signal covariance matrix is prewhitened by the estimated noise covariance, which can overcome the biased estimate of signal covariance. Finally, the performance improvement is verified by simulations in terms of resolution ability and estimation accuracy.

1. Introduction

Direction-of-arrival (DOA) estimation is one of the most important research topics in the field of array signal processing and has been widely used in the radar, sonar, wireless communications, and acoustic tracking, to mention just a few [1–6]. Resolution ability and estimation accuracy, as the two main indicators for measuring the estimation performance, have been the consistent research focus. Over the past decades, there exist several high-resolution DOA estimation approaches. Among these approaches, the most popular approaches include minimum variance distortionless response beamformer (MVDR) [7], multiple signal classification (MUSIC) [8, 9], estimation of signal parameters via rotational invariance technique (ESPRIT) [10], and maximum likelihood (ML) [11, 12]. These approaches can provide high accuracy and high resolution for DOA estimation.

For the abovementioned DOA methods, a fundamental assumption is that the DOA estimation methods are implemented in the presence of spatially uniform noise (Gaussian white noise). Under this assumption, the subspace-based approaches can successfully separate the orthogonally signal and noise subspaces, and the ML function with respect to the noise variance single parameter becomes possible [13]. In practical situations, the spatially uniform white noise can hardly be guaranteed. Except for uniform noise, the sensor noise can also be nonuniform [14], spatially correlated [15], or burst impulsive [16]. Since the array response and receive channels are usually nonideal and nonuniform, the practical noise powers across the array are nonidentical and usually behave as nonuniform [17]. The nonuniform noise usually leads to diagonal covariance matrix with nonidentical entries, which may degrade the estimation accuracy for traditional DOA estimation methods. To address this issue, the ML-based methods can deal with the nonuniform case in DOA estimation. In [18, 19], two ML-based estimators are proposed, respectively, based on iterative optimization. However, the iterative optimization procedure results in high complexity and is time-consuming. Moreover, the obtained result may be a local optimum rather than a global one [14]. For subspace-based approaches, there exist several methods to address the nonuniform noise issue [20, 21], which can avoid the iterative optimization procedure, and as a result, they are usually computationally efficient.

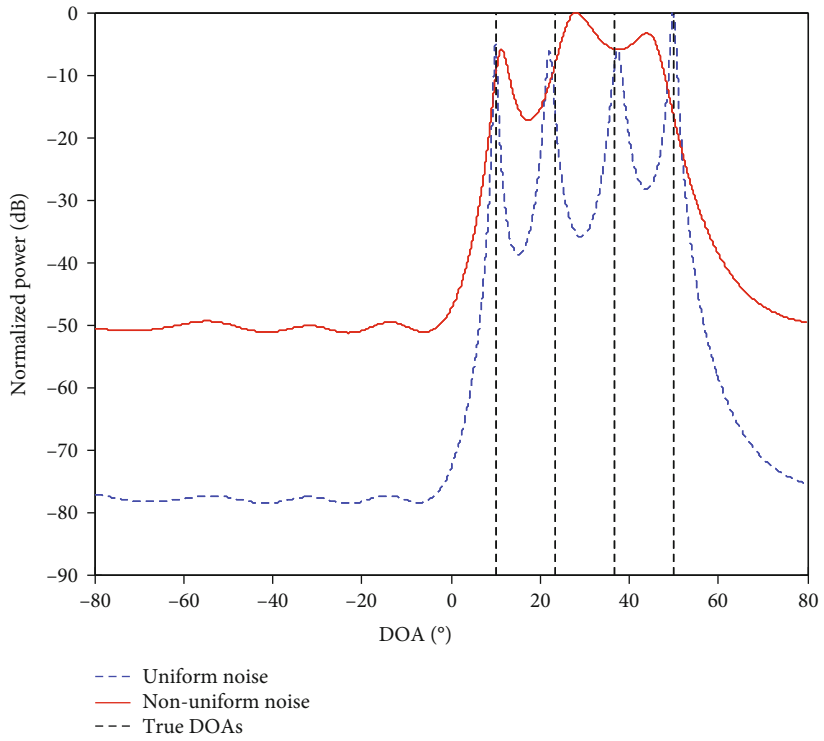

Figure 1: The MUSIC spectrum under uniform and nonuniform noises. Results with four signals arriving at angles equally distributed between 10° and 50°, $M = 8$, $L = 500$, SNR = 0 dB, and $\mathbf{q} = [1, 1, 1, 1, 1, 20, 30, 50]^T$.

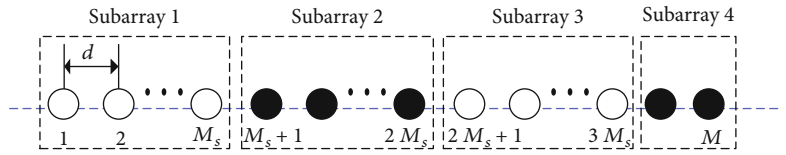

Figure 2: The ULA geometry and its subarrays.

In this paper, we propose a simple subspace-based DOA estimation method under the nonuniform noises scenarios, where the noise covariance matrix is estimated by utilizing the shift property of identical uniform subarrays, and then, some high-resolution approaches (such as MUSIC and root-MUSIC [22]) are adopted for the following DOA estimation. Simulations are provided to verify the performance improvement of the proposed method in terms of estimation accuracy and resolution ability.

2. System Model

In this section, we consider a uniform linear array (ULA) with M sensors, and the i-th sensor is located at the position $l_i = (i-1)d, i = 1, 2, \cdots, M$, where $d = \lambda/2$ and λ is the signal wavelength. Assume K far-filed uncorrelated sources impinge on the array from distinct directions $\boldsymbol{\Theta} = [\theta_1, \theta_2, \cdots, \theta_K]$. Therefore, the received signal of the array at time $t (1 \le t \le T)$ is computed as

$$\mathbf{x}(t) = \sum_{k=1}^{K} \mathbf{a}(\theta_k) s_k(t) + \mathbf{n}(t) = \mathbf{A}\mathbf{s}(t) + \mathbf{n}(t), \quad (1)$$

where $\mathbf{A} = [\mathbf{a}(\theta_1), \mathbf{a}(\theta_2), \cdots, \mathbf{a}(\theta_K)]$ is the M-by-K array manifold matrix with $\mathbf{a}(\theta_k)$ being the $M \times 1$ steering vector for the k-th signal, and the i-th element in $\mathbf{a}(\theta_k)$ is denoted as $e^{j\pi(i-1)\sin\theta_k}$. $\mathbf{s}(t) = [s_1(t), s_2(t), \cdots, s_K(t)]^T$ denotes the source signal vector at time t with the subscript T being the transpose operation. $\mathbf{n}(t)$ is the $M \times 1$ noise vector received by the array, which is uncorrelated with the signal vector $\mathbf{s}(t)$. In general, the noise $\mathbf{n}(t)$ is usually assumed as the additive white Gaussian with zero mean and variance σ^2. Under this assumption, the covariance matrix of $\mathbf{x}(t)$ can be obtained as

$$\mathbf{R}_{xx} = \mathrm{E}\left[\mathbf{x}(t)\mathbf{x}^H(t)\right] = \mathbf{A}\mathbf{R}_{ss}\mathbf{A}^H + \sigma^2\mathbf{I}_M, \quad (2)$$

where the subscript H denotes the conjugate transpose operation, $\mathrm{E}[\cdot]$ denotes expectation operation, $\mathbf{R}_{ss} = \mathrm{E}[\mathbf{s}(t)\mathbf{s}^H(t)]$ represents the signal covariance matrix of sources, and $\mathbf{I}_M$ is the M-by-M unit matrix.

In practice, the noise $\mathbf{n}(t)$ is usually nonuniform; i.e., the noises at different sensors have different noise powers. We have

$$\mathbf{Q} = E\left\{\mathbf{n}(t)\mathbf{n}(t)^H\right\} = \mathrm{diag}\,(\mathbf{q}) = \mathrm{diag}\left(\sigma_1^2, \sigma_2^2, \cdots, \sigma_M^2\right), \quad (3)$$

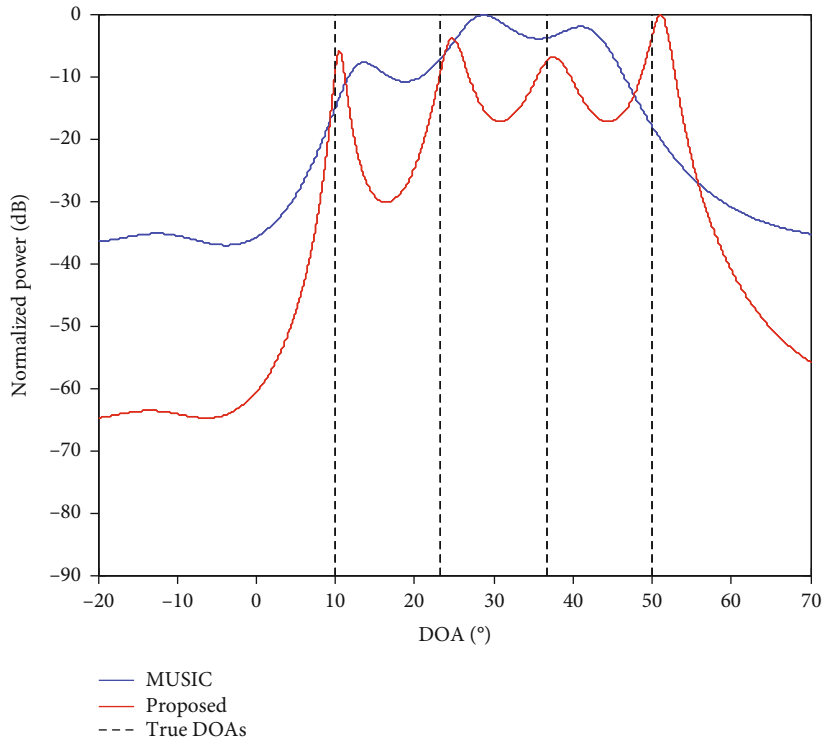

(a) SNR = −5 dB

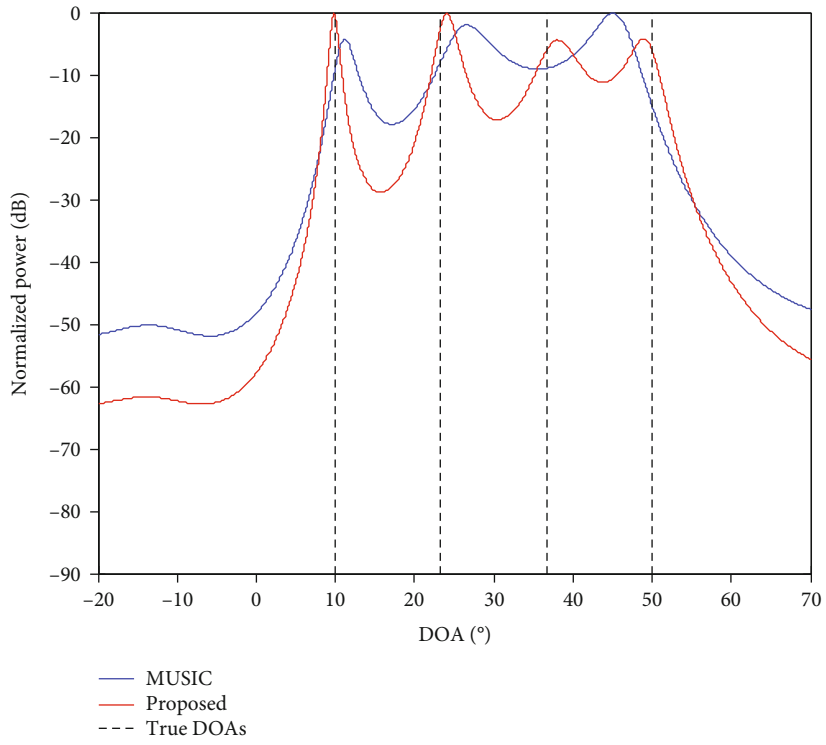

(b) SNR = 0 dB

Figure 3: Continued.

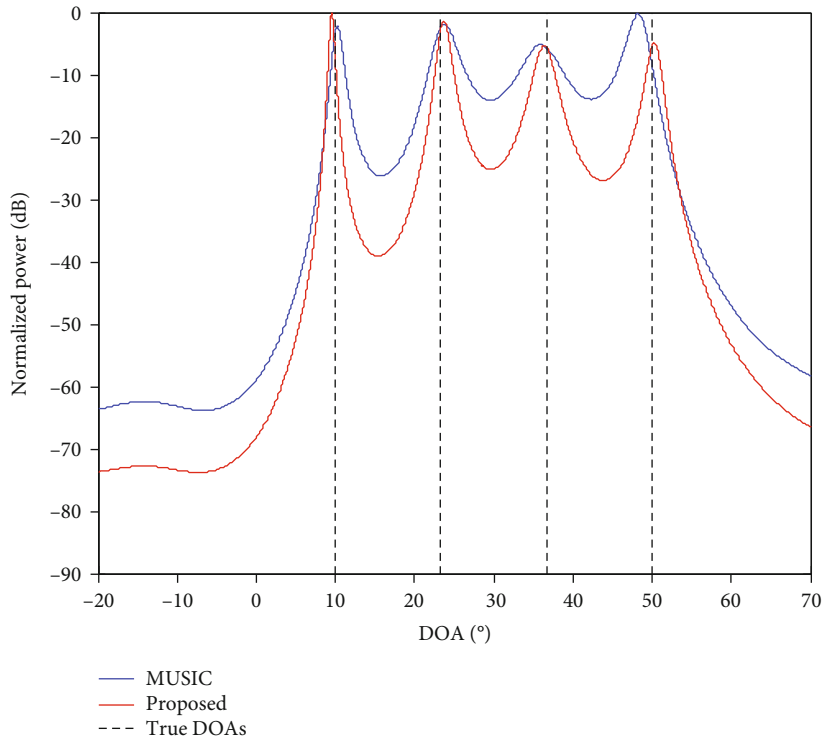

(c) SNR = 5 dB

FIGURE 3: The normalized spectrum under different SNRs with (a) SNR = −5 dB, (b) 0 dB, and (c) 5 dB. Results with four signals arriving at angles equally distributed between 10° and 50°, $M = 8$, and $L = 500$.

where σ_i^2, $i = 1, 2, \cdots, M$ is the sensor noise covariance at the i -th sensor with $\mathbf{q} = [\sigma_1^2, \sigma_2^2, \cdots, \sigma_M^2]^T$ and diag $(\cdot)$ denotes a diagonal matrix. In this case, the covariance matrix of $\mathbf{x}(t)$ becomes

$$\mathbf{R}_{xx} = \mathrm{E}\left[\mathbf{x}(t)\mathbf{x}^H(t)\right] = \mathbf{A}\mathbf{R}_{ss}\mathbf{A}^H + \mathbf{Q}. \tag{4}$$

From Equations (2) and (4), the uniform noise can be regarded as a special case of nonuniform noise when $\sigma_1^2 = \sigma_2^2 = \cdots = \sigma_M^2 = \sigma^2$, i.e., $\mathbf{Q} = \sigma^2\mathbf{I}_M$.

Due to the effect of limited samples, the covariance matrix $\mathbf{R}_{xx}$ is unavailable, but it can be estimated with L snapshots as

$$\widehat{\mathbf{R}}_{xx} = \frac{1}{L}\sum_{t=1}^{L}\mathbf{x}(t)\mathbf{x}^H(t), \tag{5}$$

where the estimated covariance matrix $\widehat{\mathbf{R}}_{xx}$ converges to $\mathbf{R}_{xx}$ when the snapshot number L tends to be large enough. The eigenvalue decomposition can be written as

$$\widehat{\mathbf{R}}_{xx} = \mathbf{U}_s\mathbf{\Lambda}_s\mathbf{U}_s^H + \mathbf{U}_n\mathbf{\Lambda}_n\mathbf{U}_n^H, \tag{6}$$

where $\mathbf{U}_s$ and $\mathbf{U}_n$ are the spanned signal and noise subspace and $\mathbf{\Lambda}_s$ and $\mathbf{\Lambda}_n$ are the corresponding eigenvalue matrices with respect to $\mathbf{U}_s$ and $\mathbf{U}_n$, respectively. The pseudospectrum of MUSIC can be obtained as

$$f(\theta) = \frac{1}{\mathbf{a}^H(\theta)\mathbf{U}_n\mathbf{U}_n^H\mathbf{a}(\theta)}. \tag{7}$$

Then, the DOAs can be estimated by finding the peaks of $f(\theta)$. However, as compared to the uniform noise scenarios, the nonuniform noise may interrupt the MUSIC spectrum and degrade the estimation performance. For clarity, we give an example of the MUSIC spectrum under both uniform and nonuniform noises in Figure 1. Here, we consider $K = 4$ uncorrelated sources equally distributed between 10° and 50° impinge on the ULA with $M = 8$, $L = 500$, and the SNR being 0 dB. For the nonuniform noise case, the noise power vector is set as $\mathbf{q} = [1, 1, 1, 1, 1, 20, 30, 50]^T$. As can be observed from Figure 1, the MUSIC spectrum performs well under the uniform noise case. Meanwhile, under the nonuniform noise scenarios, the MUSIC can only generate three peaks with larger error and missing one source, which indicates that the conventional MUSIC may become invalid for nonuniform noise cases.

3. Proposed Method

For an M-element ULA, it can be divided into three consecutive subarrays with the same aperture and no overlapping

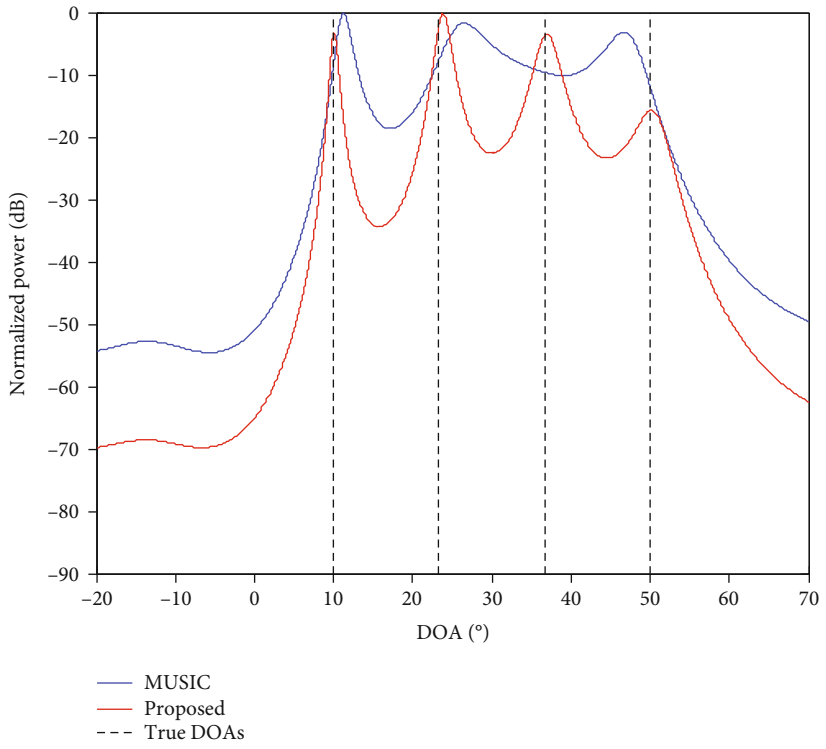

(a) WNPR = 10

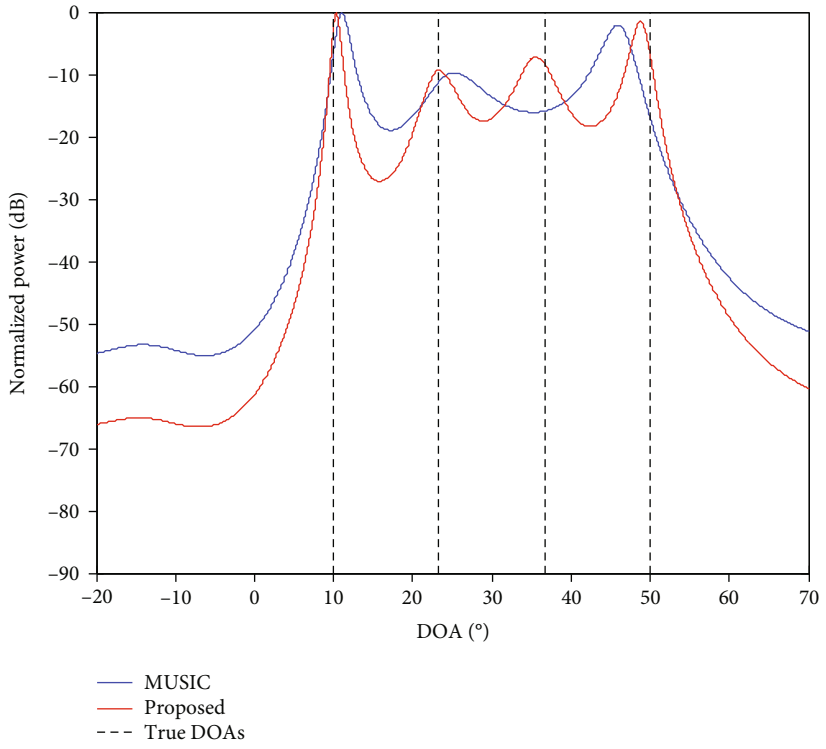

(b) WNPR = 30

Figure 4: Continued.

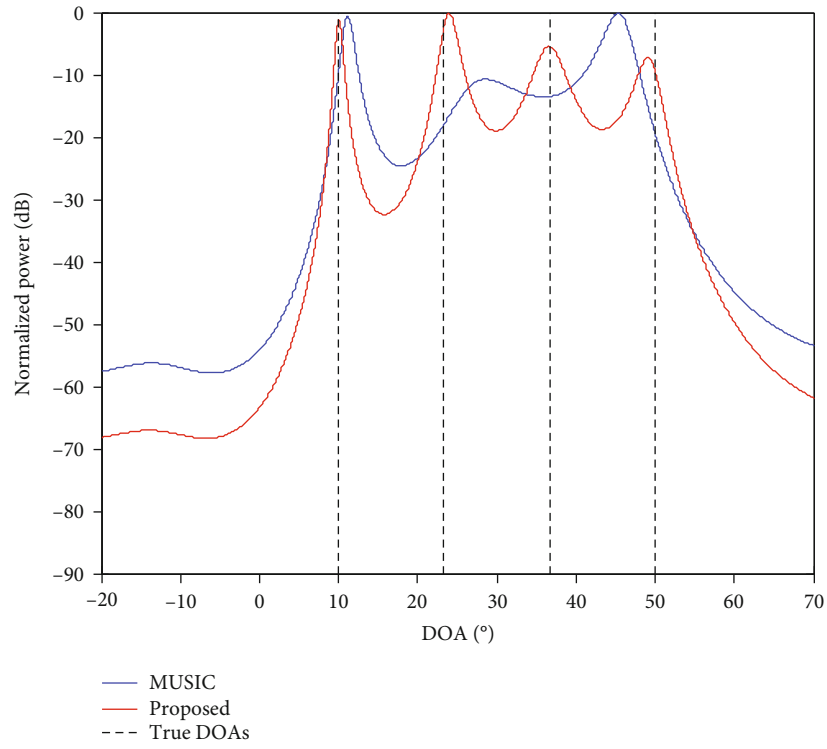

(c) WNPR = 50

FIGURE 4: The normalized spectrum under different WNPRs with (a) WNPR = 10, (b) 30, and (c) 50. Results with four signals arriving at angles equally distributed between 10° and 50°, $M = 8$, and SNR = 0 dB.

elements, as is shown in Figure 2. Each subarray is a uniform linear subarray with M_s elements, where $M_s = \lfloor M/3 \rfloor$ with the symbol $\lfloor \cdot \rfloor$ being the round down to the nearest integral operation. The remaining elements can be regarded as the fourth subarray with $M_r = M - 3M_s$ elements and M_r can be 0, 1, or 2. Note that when $M_r = 0$, the fourth subarray does not exist, i.e., the fourth subarray exists only when $M \neq 3M_s$.

Without loss of generality, the covariance matrices of the four subarrays can be extracted directly from $\mathbf{R}_{xx}$ in Equation (4) as

$$\begin{cases} \mathbf{R}_{xx,1} = \mathbf{R}_{xx}(1 : M_s ; 1 : M_s) = \mathbf{A}_1 \mathbf{R}_{ss} \mathbf{A}_1{}^H + \mathbf{Q}_1, \\ \mathbf{R}_{xx,2} = \mathbf{R}_{xx}(M_s + 1 : 2M_s ; M_s + 1 : 2M_s) = \mathbf{A}_2 \mathbf{R}_{ss} \mathbf{A}_2{}^H + \mathbf{Q}_2, \\ \mathbf{R}_{xx,3} = \mathbf{R}_{xx}(2M_s + 1 : 3M_s ; 2M_s + 1 : 3M_s) = \mathbf{A}_3 \mathbf{R}_{ss} \mathbf{A}_3{}^H + \mathbf{Q}_3, \\ \mathbf{R}_{xx,4} = \mathbf{R}_{xx}(3M_s + 1 : M ; 3M_s + 1 : M) = \mathbf{A}_4 \mathbf{R}_{ss} \mathbf{A}_4{}^H + \mathbf{Q}_4, \end{cases} \tag{8}$$

where $\mathbf{A}_1$, $\mathbf{A}_2$, and $\mathbf{A}_3$ are the M_s-by-K array manifold matrices of the former three subarrays extracted from $\mathbf{A}$ and satisfy $\mathbf{A}_{i+1} = \mathbf{F}\mathbf{A}_i$ with $\mathbf{F} = \text{diag}([e^{j\pi(1+M_s)\sin\theta_1}, \cdots, e^{j\pi(1+M_s)\sin\theta_K}])$ for $i = 1, 2$. $\mathbf{A}_4$ is the M_r-by-K array manifold matrix for the fourth subarray. $\mathbf{Q}_1 = \text{diag}(\mathbf{q}(1 : M_s))$, $\mathbf{Q}_2 = \text{diag}(\mathbf{q}(1 + M_s : 2M_s))$, $\mathbf{Q}_3 = \text{diag}(\mathbf{q}(1 + 2M_s : 3M_s))$, and $\mathbf{Q}_4 = \text{diag}(\mathbf{q}(3M_s + 1 : M))$. From Equation (8), $\mathbf{A}_i \mathbf{R}_{ss} \mathbf{A}_i{}^H$ $(i = 1, 2, 3, 4)$ can be regarded as the noise-free covariance matrix.

For the former three subarrays, they are identical subarrays with different origin shifts. Since $\mathbf{A}_i = \mathbf{F}\mathbf{A}_{i-1}$ holds for $(i = 2, 3)$ and $\mathbf{F}$ and $\mathbf{R}_{ss}$ are both diagonal matrices, the noise-free covariance $\mathbf{A}_i \mathbf{R}_{ss} \mathbf{A}_i{}^H$ can be simplified as $\mathbf{A}_i \mathbf{R}_{ss} \mathbf{A}_i{}^H = \mathbf{A}_1 \mathbf{F}^{(i-1)} \mathbf{R}_{ss} (\mathbf{F}^{(i-1)})^H \mathbf{A}_1{}^H = \mathbf{A}_1 \mathbf{R}_{ss} \mathbf{A}_1{}^H$. Equivalently, the noise-free covariance matrices of the three former subarrays are approximately the same, which can be utilized to eliminate the effect of nonuniform noise.

The cross-covariance matrices for the former three subarrays can be obtained in a similar approach as

$$\begin{cases} \mathbf{C}_{12} = \mathbf{R}_{xx}(1 : M_s ; M_s + 1 : 2M_s) = \mathbf{A}_1 \mathbf{R}_{ss} \mathbf{A}_2{}^H, \\ \mathbf{C}_{13} = \mathbf{R}_{xx}(1 : M_s ; 2M_s + 1 : 3M_s) = \mathbf{A}_1 \mathbf{R}_{ss} \mathbf{A}_3{}^H, \\ \mathbf{C}_{23} = \mathbf{R}_{xx}(M_s + 1 : 2M_s ; 2M_s + 1 : 3M_s) = \mathbf{A}_2 \mathbf{R}_{ss} \mathbf{A}_3{}^H, \end{cases} \tag{9}$$

where $\mathbf{C}_{ij}$ $(i, j = 1, 2, 3,\ i \neq j)$ denotes the cross-covariance matrix between the i-th subarray and j-th subarray. According to the definition of cross-covariance matrix, $\mathbf{C}_{ij} = \mathbf{C}_{ji}^H$ holds. Note that the cross-covariance matrices do not contain the noise item since the noises are uncorrelated with the signal and are mutually uncorrelated at different sensors.

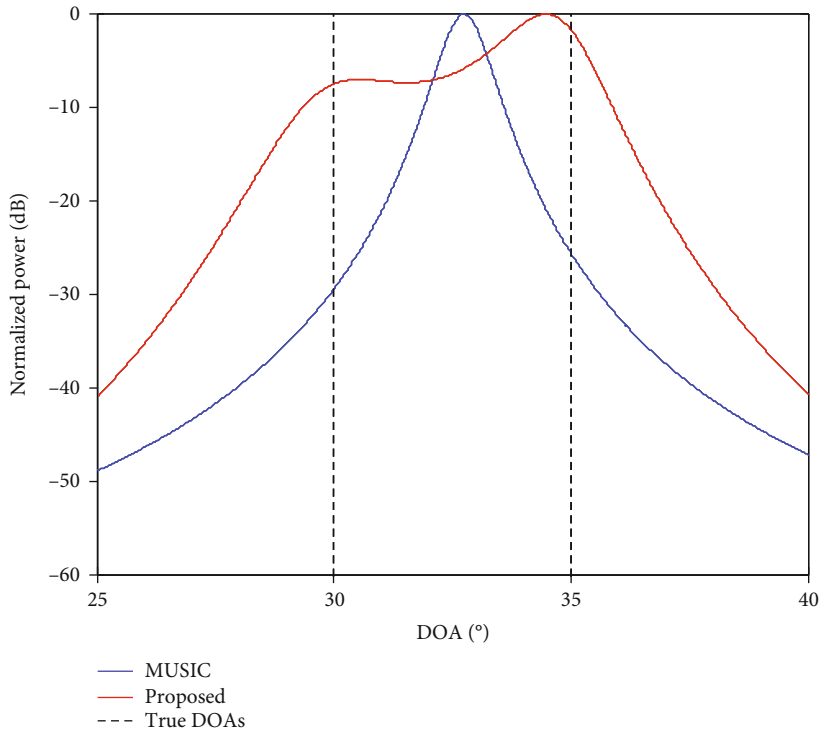

(a) SNR = 0 dB

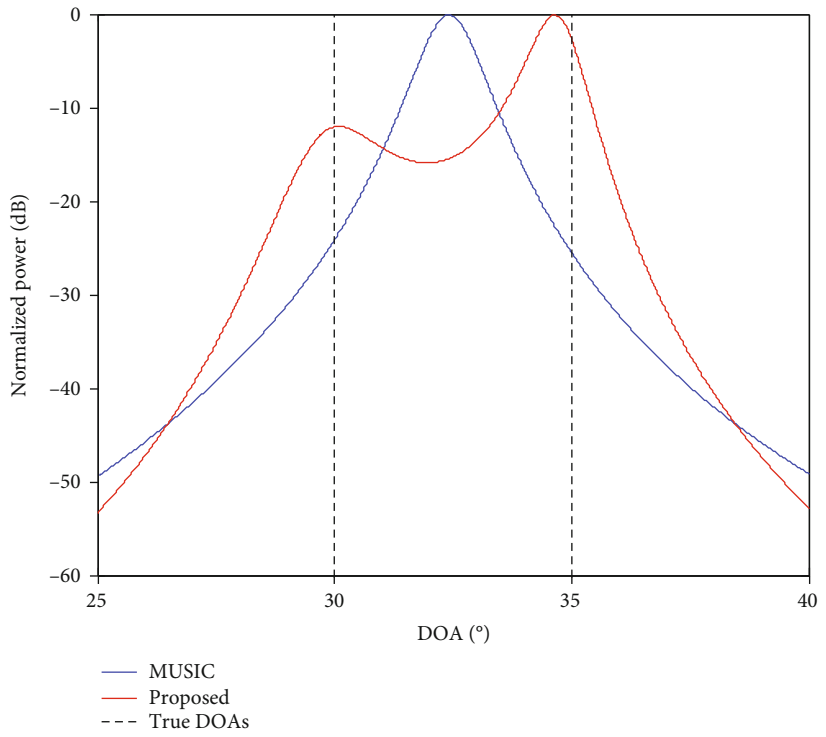

(b) SNR = 5 dB

Figure 5: Continued.

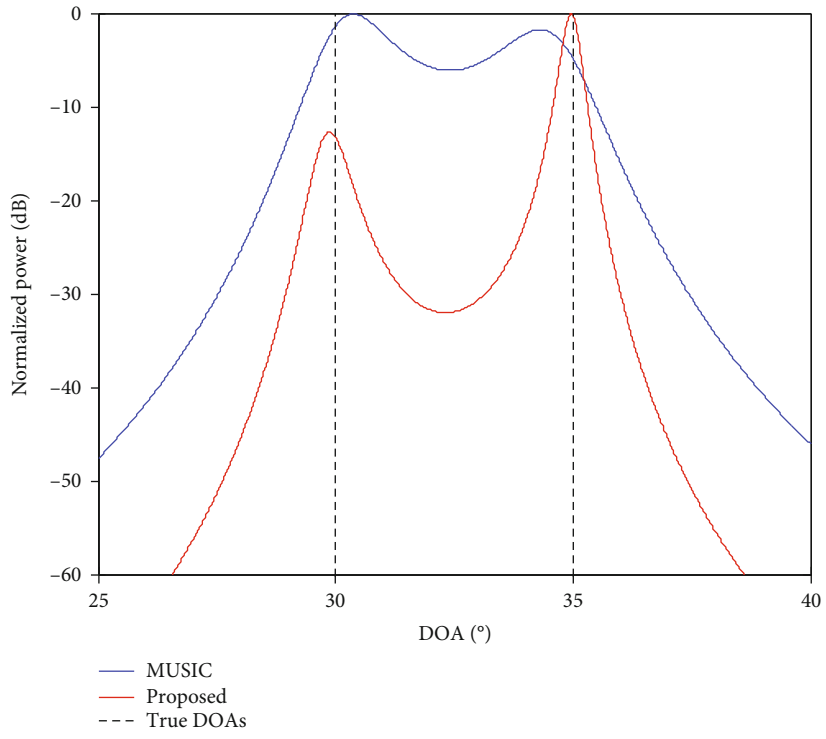

(c) SNR = 10 dB

FIGURE 5: The normalized spectrum under different SNRs with (a) SNR = 0 dB, (b) 5 dB, and (c) 10 dB. Results with two closely located signals arriving at angles 30° and 35°, $M = 8$, and $L = 500$.

We can define two new matrices as

$$\begin{cases} \mathbf{T}_1 = \mathbf{C}_{12}^{-1}\mathbf{R}_{xx,1} = \left(\mathbf{A}_1\mathbf{R}_{ss}\mathbf{A}_2{}^H\right)^{-1}\left(\mathbf{A}_1\mathbf{R}_{ss}\mathbf{A}_1{}^H + \mathbf{Q}_1\right), \\ \mathbf{U}_1 = \mathbf{C}_{13}^{-1}\mathbf{C}_{12} = \left(\mathbf{A}_1\mathbf{R}_{ss}\mathbf{A}_3{}^H\right)^{-1}\left(\mathbf{A}_1\mathbf{R}_{ss}\mathbf{A}_2{}^H\right), \end{cases} \tag{10}$$

where $(\cdot)^{-1}$ denotes the matrix inverse operation. According to the relationship of $\mathbf{A}_1$, $\mathbf{A}_2$, and $\mathbf{A}_3$, we can simplify Equation (10) as $\mathbf{T}_1 = \mathbf{F} + \mathbf{C}_{12}^{-1}\mathbf{Q}_1$ and $\mathbf{U}_1 = \mathbf{F}$, and thus, we have

$$\mathbf{T}_1 - \mathbf{U}_1 = \mathbf{C}_{12}^{-1}\mathbf{Q}_1. \tag{11}$$

From Equation (11), $\mathbf{Q}_1$ can be estimated as

$$\hat{\mathbf{Q}}_1 = \mathbf{C}_{12}(\mathbf{T}_1 - \mathbf{U}_1) = \mathbf{R}_{xx,1} - \mathbf{C}_{12}\mathbf{C}_{13}^{-1}\mathbf{C}_{12}. \tag{12}$$

Similarly, by defining

$$\begin{cases} \mathbf{T}_3 = \left(\mathbf{C}_{23}^H\right)^{-1}\mathbf{R}_{xx,3} = \left(\mathbf{A}_3\mathbf{R}_{ss}\mathbf{A}_2{}^H\right)^{-1}\left(\mathbf{A}_3\mathbf{R}_{ss}\mathbf{A}_3{}^H + \mathbf{Q}_3\right) = \mathbf{F}^H + \left(\mathbf{C}_{23}^H\right)^{-1}\mathbf{Q}_3, \\ \mathbf{U}_3 = \left(\mathbf{C}_{13}^H\right)^{-1}\mathbf{C}_{23}^H = \left(\mathbf{A}_3\mathbf{R}_{ss}\mathbf{A}_1{}^H\right)^{-1}\left(\mathbf{A}_3\mathbf{R}_{ss}\mathbf{A}_2{}^H\right) = \mathbf{F}^H. \end{cases} \tag{13}$$

And $\mathbf{Q}_3$ can be estimated as

$$\hat{\mathbf{Q}}_3 = \mathbf{C}_{23}^H(\mathbf{T}_3 - \mathbf{U}_3). \tag{14}$$

With the estimated $\hat{\mathbf{Q}}_1$ and $\hat{\mathbf{Q}}_3$, the corresponding noise-free estimated covariance matrices for $\mathbf{R}_{xx,1}$ and $\mathbf{R}_{xx,3}$ are

$$\begin{cases} \hat{\mathbf{R}}_{xx,1} = \mathbf{R}_{xx,1} - \hat{\mathbf{Q}}_1 \approx \mathbf{A}_1\mathbf{R}_{ss}\mathbf{A}_1{}^H, \\ \hat{\mathbf{R}}_{xx,3} = \mathbf{R}_{xx,3} - \hat{\mathbf{Q}}_3 \approx \mathbf{A}_3\mathbf{R}_{ss}\mathbf{A}_3{}^H. \end{cases} \tag{15}$$

Since the noise-free covariance matrices of the former three subarrays are approximately the same, then we can estimate $\mathbf{Q}_2$ as

$$\hat{\mathbf{Q}}_2 = \frac{\mathbf{R}_{xx,2} - \left(\hat{\mathbf{R}}_{xx,1} + \hat{\mathbf{R}}_{xx,3}\right)}{2}. \tag{16}$$

In the following, we will estimate the noise power matrix for the fourth subarray, which can be categorised into two cases.

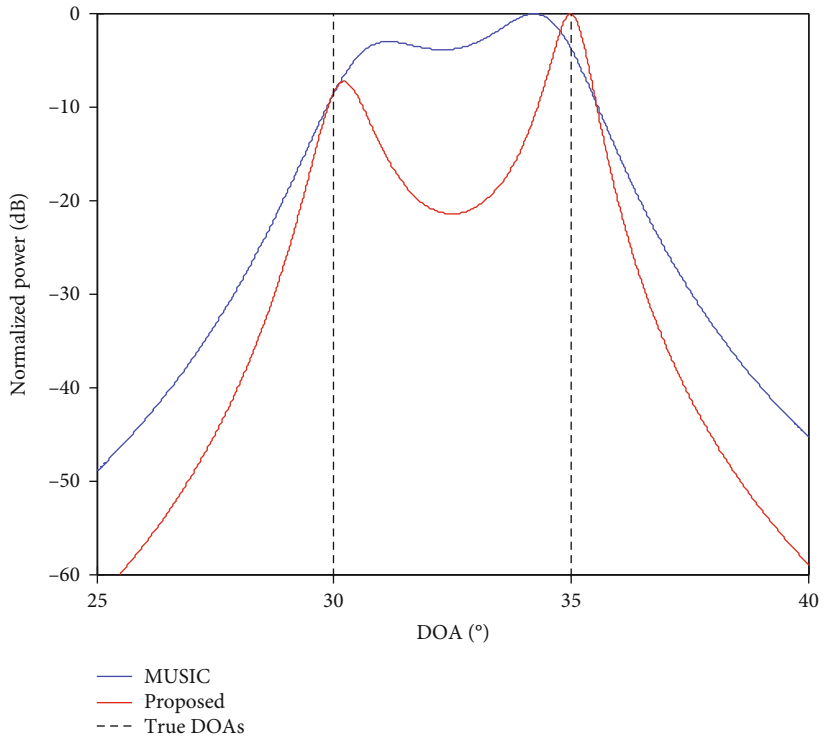

(a) WNPR =10

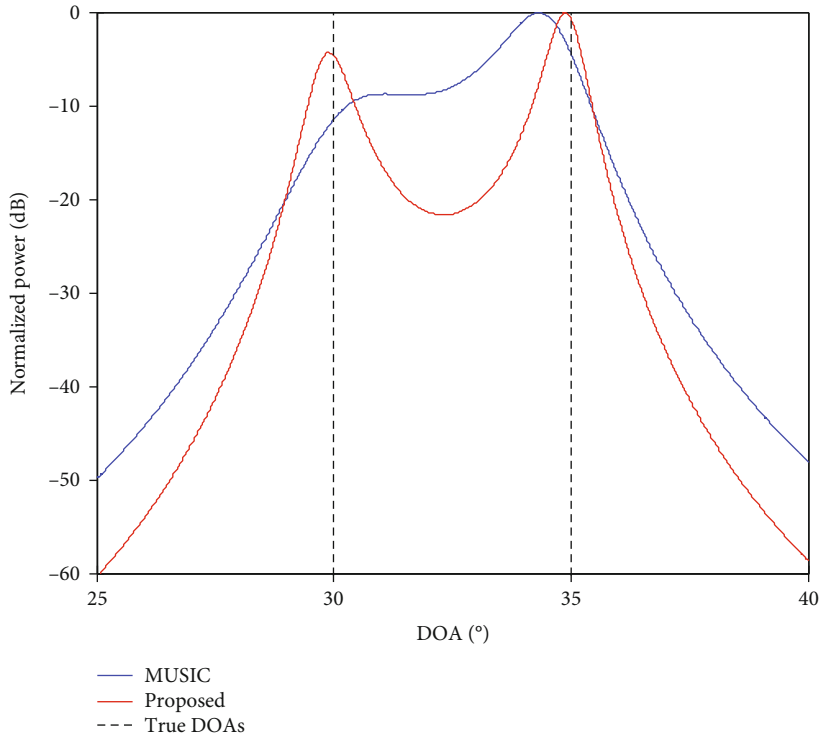

(b) WNPR = 30

Figure 6: Continued.

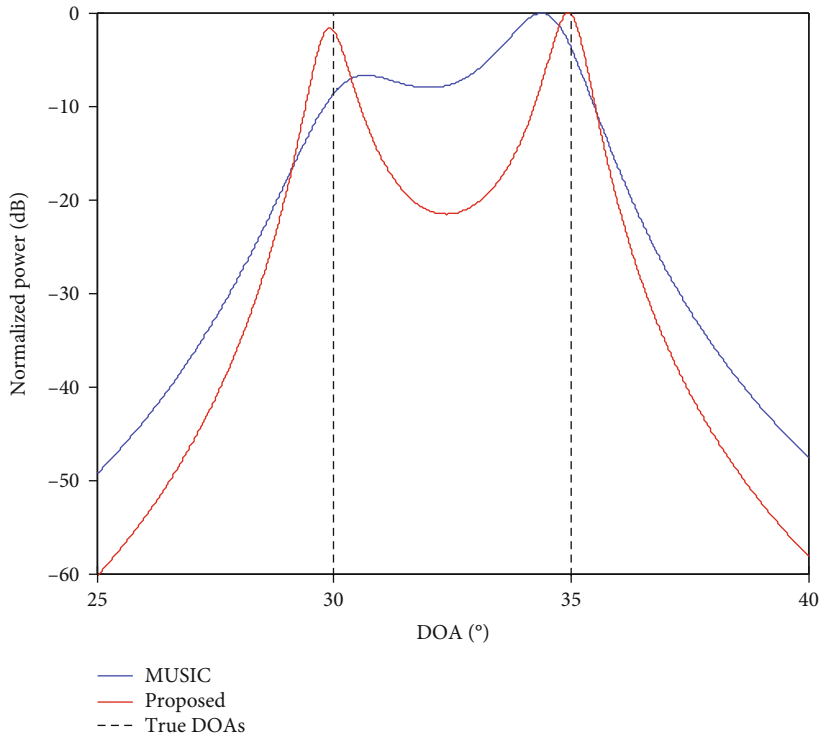

(c) WNPR = 50

FIGURE 6: The normalized spectrum under different WNPRs with (a) WNPR = 10, (b) 30, and (c) 50. Results with two closely located signals arriving at angles 30° and 35°, $M = 8$, and SNR = 10 dB.

Case 1. When $M_r = 0$, the fourth subarray does not exist.

With the estimated $\hat{\mathbf{Q}}_1$, $\hat{\mathbf{Q}}_2$, and $\hat{\mathbf{Q}}_3$, the noise-free covariance matrix can be obtained correspondingly, i.e.,

$$\hat{\mathbf{R}}_{xx,nf}^{(1)} = \hat{\mathbf{R}}_{xx} - \text{diag}\,(\hat{\mathbf{q}}_{13}), \tag{17}$$

where $\hat{\mathbf{q}}_{13} = [\text{diag}\,(\hat{\mathbf{Q}}_1), \text{diag}\,(\hat{\mathbf{Q}}_2), \text{diag}\,(\hat{\mathbf{Q}}_3)]$.

Case 2. When $M_r \neq 0$, the fourth subarray exists.

The fourth subarray contains M_r elements, and its covariance matrix is $\mathbf{R}_{xx,4}$ in Equation (8). As the noise-free covariance matrices of identical ULAs with different shifts are the same, we can divide $\hat{\mathbf{R}}_{xx,nf}^{(1)}$ into $N = \lfloor 3M_s/M_r \rfloor$ parts, which are identical with the fourth subarray with different shifts and no overlapping. And the covariance matrix of the n-th $(n = 1, 2, \cdots, N)$ part is

$$\hat{\mathbf{R}}_{n,\text{free}} = \hat{\mathbf{R}}_{xx,nf}^{(1)}((n-1)M_r + 1 : nM_r\,; (n-1)M_r + 1 : nM_r). \tag{18}$$

According to the shift property of identical subarrays, the noise-free covariance matrix of the fourth subarray and $\hat{\mathbf{R}}_{n,\text{free}}$ is the same. $\mathbf{Q}_4$ can be estimated as

$$\hat{\mathbf{Q}}_4 = \mathbf{R}_{xx,4} - \frac{1}{N}\sum_{n=1}^{N} \hat{\mathbf{R}}_{n,\text{free}}. \tag{19}$$

Then, we can obtain the noise-free covariance matrix of the entire array for Case 2 as

$$\hat{\mathbf{R}}_{xx,nf}^{(2)} = \hat{\mathbf{R}}_{xx} - \text{diag}\,(\hat{\mathbf{q}}_{14}), \tag{20}$$

where $\hat{\mathbf{q}}_{14} = [\text{diag}\,(\hat{\mathbf{Q}}_1), \text{diag}\,(\hat{\mathbf{Q}}_2), \text{diag}\,(\hat{\mathbf{Q}}_3), \text{diag}\,(\hat{\mathbf{Q}}_4)]$.

Therefore, from Equations (12), (14), (16), and (19), an estimation of the noise-covariance matrix is obtained by the estimation of $\mathbf{Q}_1$, $\mathbf{Q}_2$, $\mathbf{Q}_3$, and $\mathbf{Q}_4$. Using the estimated noise-covariance matrix, we can prewhiten the received array data and obtain the noise-free covariance matrix, in Equations (17) and (20) for different cases. Then, DOAs can be estimated by several classic approaches, such as MUSIC and root-MUSIC.

As depicted above, the proposed approach firstly estimates the noise covariance matrix to obtain the noise-free covariance matrix and then uses some classical approaches for the following DOA estimation. Therefore, the complexity mainly includes two parts: the estimation of noise-covariance matrix and the estimation of DOAs by classical approaches. For the estimation of noise-covariance matrix, it mainly involves the calculation of covariance matrix $\mathbf{R}_{xx}$ and the estimation of noise covariance matrix; the complexities of which are $\mathcal{O}(M^2L)$ and $\mathcal{O}(6M_s^3)$, respectively. For the classical DOA estimation approaches, such as MUSIC and root-MUSIC, their complexities can be approximately denoted as $\mathcal{O}(M^2S)$ [23] and $\mathcal{O}(20M^2K)$ [24], where $S(\gg L)$ denotes the number of spectral points of the total angular field of view. In general, by applying the proposed approach

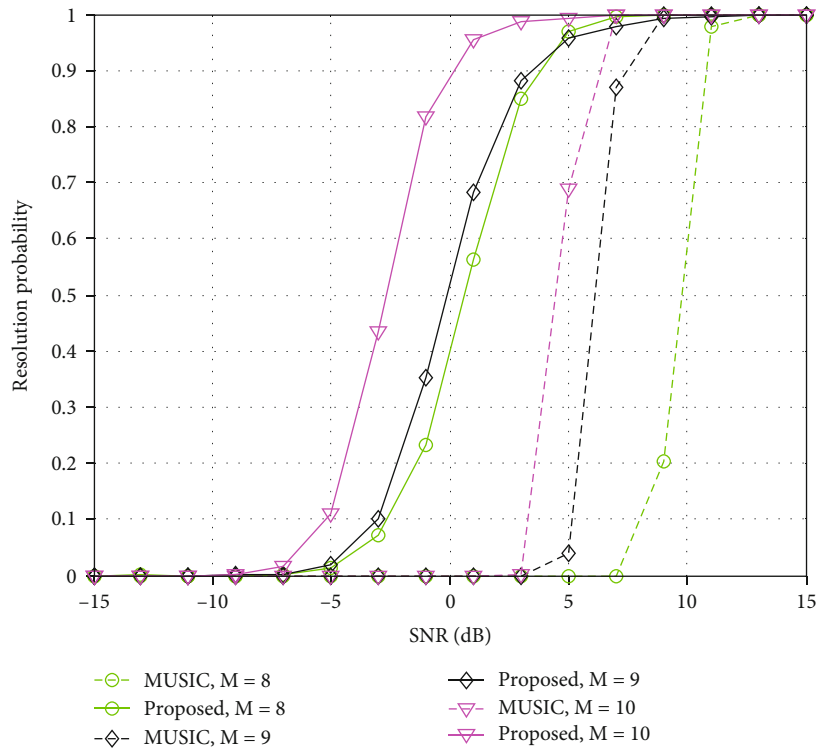

(a) Resolution probability vs. SNR

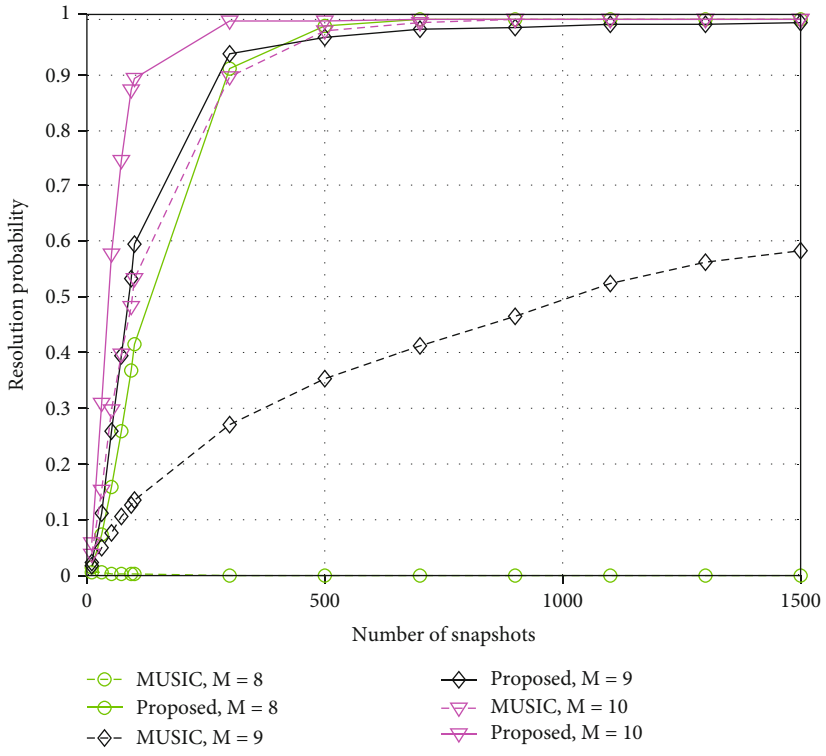

(b) Resolution probability vs. snapshot number

Figure 7: Continued.

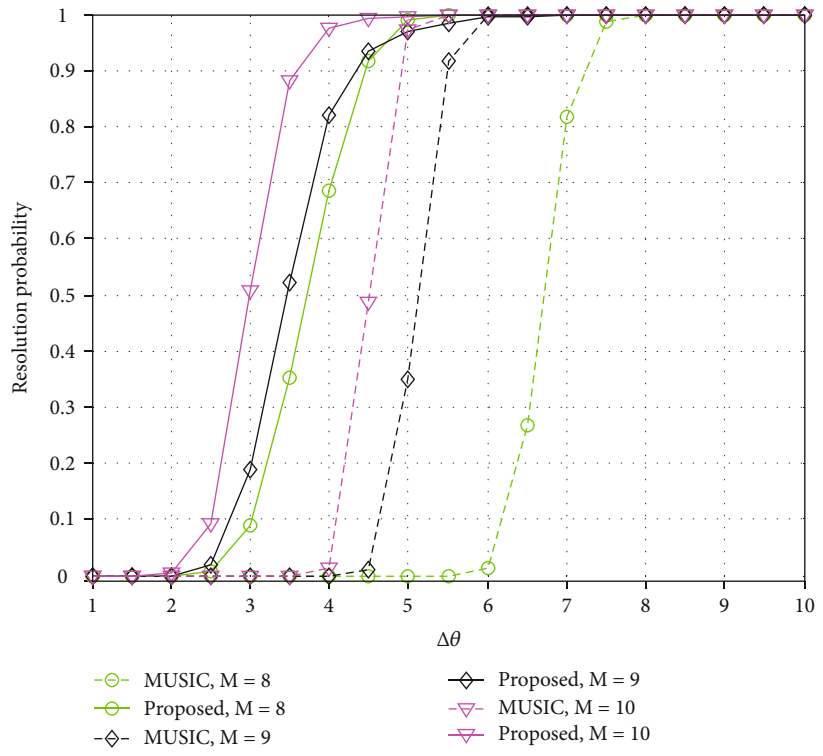

(c) Resolution probability vs. angular difference $\Delta\theta$

FIGURE 7: The resolution probability of different approaches under $M = 8$, 9, and 10 sensors with respect to (a) SNR, (b) snapshot number, and angular difference $\Delta\theta$. Results with two closely located signals arriving at angles 30° and 35°. Other conditions include (a) $L = 500$, (b) SNR = 6 dB, and (c) SNR = 6 dB, $L = 500$, and $\theta_1 = 30°$.

to MUSIC and root-MUSIC, the complexities become $\mathcal{O}(M^2S + M^2L + 6M_s^3)$ and $\mathcal{O}(20M^2K + M^2L + 6M_s^3)$, respectively. As compared to the original estimation approach, the complexities become slightly larger. However, the performance can be greatly improved, which is verified by the following numerical results.

4. Results and Discussion

In this section, we evaluate the performance of the proposed method via simulations. The worst noise power ratio (WNPR) is defined as $\text{WNPR} = \sigma_{\max}^2/\sigma_{\min}^2$ and the signal-to-noise ratio (SNR) is defined as $\text{SNR} = \sigma_s^2/\sum_{k=1}^{K}\sigma_k^2/K$, where $\sigma_{\max}^2$ and $\sigma_{\min}^2$ denote the maximum and minimum noise powers, respectively, and σ_s^2 is the signal power. The root mean squared error (RMSE), defined as $\text{RMSE} = (1/KL)\sqrt{\sum_{k=1}^{K}\sum_{j=1}^{J}(\widehat{\theta}_{k,j} - \theta_k)^2}$, is adopted as the performance criteria, where $\widehat{\theta}_{k,j}$ denotes the estimate of the k-th DOA in the j-th trial.

The effectiveness and robustness of the proposed approach are firstly verified. Here, we consider $K = 4$ sources equally distributed between 10° and50°. The ULA is modelled with $M = 8$ sensors, and the snapshot number is set as $L = 500$. Figure 3 shows the normalized spectra of the proposed approach and MUSIC under different SNRs with $\mathbf{q} = [1, 1, 1, 1, 1, 20, 30, 50]^T$. Figure 4 shows the normalized spectra of the proposed approach and MUSIC under different WNPRs with SNR = 0 dB. As is observed, the proposed approach can generate four obvious spectral peaks under different SNRs and WNPRs, all of which are coincident with the true DOAs. Meanwhile, the MUSIC approach may generate less peaks, especially for low SNRs. And the generated peaks deviate the positions of true DOAs. With the increase of SNR, the MUSIC approach can generate four peaks, but the proposed approach still provides sharper spectra than that of the MUSIC approach. Therefore, the proposed approach can achieve effective and robust DOA estimation under different SNRs and WNPRs.

To verify the resolution performance of the proposed approach, we test our approach and MUSIC at a small angular difference. Two closely located sources are assumed to impinge on the array from DOAs 30°and35°, and other experimental conditions are kept unchanged. The spectra with different SNRs and WNPRs are shown in Figures 5 and 6, respectively. As is shown, the traditional MUSIC can generate only one spectral peak at low SNR and thus fail to distinguish the two sources. Despite the increase of SNR, the MUSIC can successfully detect the two closely located sources, but they may deviate the positions of true DOAs. In contrast, the spectrum of the proposed approach has two obvious peaks both under different SNRs and WNPRs. The DOAs corresponding to the peaks are coincident with

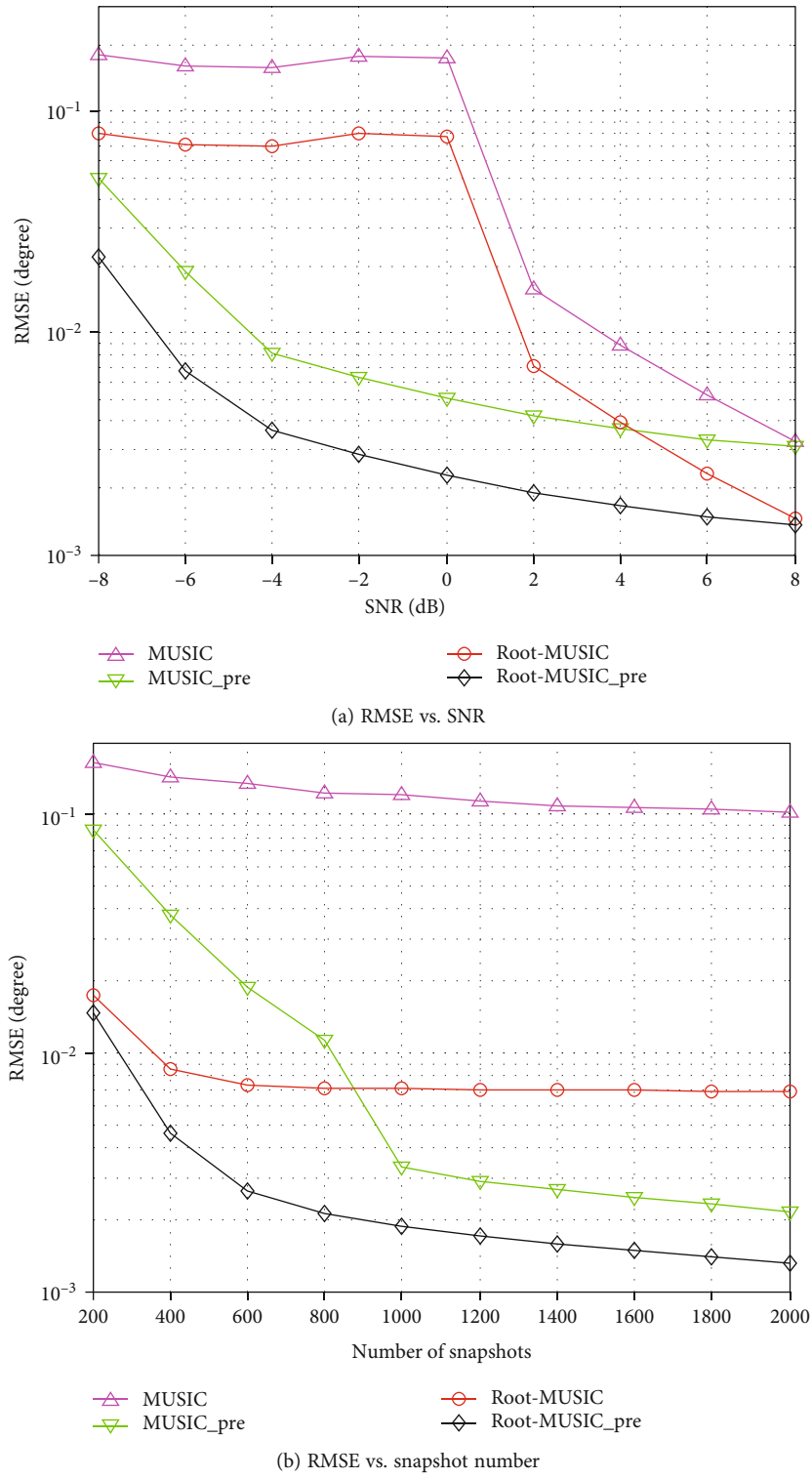

FIGURE 8: The RMSE performance of different approaches with respect to (a) SNR and (b) snapshot number. Results with four signals arriving at angles equally distributed between 10° and 50°, $M = 8$, and $L = 1000$ (a), SNR = 2 dB (b).

the true DOAs, indicating that the proposed approach can achieve effective DOA estimation of closely located DOAs under different conditions.

Subsequently, the results of resolution probability to detect two closely located sources under different SNRs, snapshot number, and angular differences are shown in Figure 7. Here, we consider the ULA with $M = 8$, 9, and 10 sensors, and two closely located sources are assumed to impinge on the array from DOAs 30° and 35° for Figures 7(a) and 7(b). Other experimental conditions are

kept unchanged. It is observed that both the proposed approach and MUSIC exhibit improved resolution probability with the increase of SNR, snapshot number, angular differences, and sensor number. At the same time, the proposed approach occupies higher resolution probability in all the considered cases and reaches 100% resolution probability much faster than that of the MUSIC method. The results in Figure 7 demonstrate the superiority of the proposed approach in terms of the resolution probability.

Furthermore, the RMSE performance under different SNRs and snapshot numbers is shown in Figure 8. Here, we consider an ULA with $M = 8$ sensors. There are $K = 4$ incident DOAs equally distributed between 10° and50°. The MUSIC and root-MUSIC approaches are adopted for comparisons, and the proposed approaches are also performed for the two traditional methods (denoted as *MUSIC_pre* and *root-MUSIC_pre*), respectively. As can be observed, the RMSE performance is improved with the increase of SNR and snapshot number. By performing the proposed prewhitening procedure, the improved approach can provide lower RMSE, especially at low SNR and larger snapshot number. The reasons are given as follows. When the SNR is low, the nonuniform noises become the dominant factor to degrade the estimation accuracy, and the proposed approach can eliminate the effect; with the increase of SNR, the nonuniform noises become less important, and the estimation performance will converge to be similar. On the other hand, with the increase of snapshot number, the estimated noise power matrix becomes more accurate, which can enhance the estimation performance of DOAs. The results in Figure 8 effectively verify the superiority of the proposed approach under different SNRS and snapshot numbers.

5. Conclusions

In this paper, we propose a simple DOA estimation method in the presence of spatially nonuniform white noise with unknown noise covariance matrix. Firstly, the unknown noise covariance matrix is estimated according to the shift property of identical subarrays. Then, the received signal covariance matrix is prewhitened by the estimated noise covariance to overcome the biased estimate of signal covariance. Therefore, the performance of the proposed method can be improved. Finally, simulation results are provided to verify the effectiveness of the proposed approach in terms of resolution ability and estimation accuracy.

Data Availability

No data were used to support this study.

Conflicts of Interest

The authors declare that there is no conflict of interest regarding the publication of this paper.

Acknowledgments

This work was partially supported by the Natural Science Foundation of Shandong Province under Grant ZR2019MF026 and the Shandong Provincial Key Research and Development Program of China under Grant 2019GNC106106.

References

[1] H. Krim and M. Viberg, "Two decades of array signal processing research: the parametric approach," *IEEE Signal Processing Magazne*, vol. 13, no. 4, pp. 67–94, 1996.

[2] P. Stoica and A. Nehorai, "Performance study of conditional and unconditional direction-of-arrival estimation," *IEEE Transactions on Acoustics Speech and Signal Processing*, vol. 38, no. 10, pp. 1783–1795, 1990.

[3] A. Olfat and S. Nader-Esfahani, "A new signal subspace processing for DOA estimation," *Signal Processing*, vol. 84, no. 4, pp. 721–728, 2004.

[4] E. Aboutanios, A. Hassanien, A. El-Keyi, Y. Nasser, and S. A. Vorobyov, "Advances in DOA estimation and source localization," *International Journal of Antennas and Propagation*, vol. 2017, Article ID 1352598, 3 pages, 2017.

[5] G. Zheng, Y. Song, and C. Chen, "Height measurement with meter wave polarimetric MIMO radar: signal model and MUSIC-like algorithm," *Signal Processing*, vol. 190, article 108344, 2022.

[6] F. Wen, J. Shi, and Z. Zhang, "Generalized spatial smoothing in bistatic EMVS-MIMO radar," *Signal Processing*, vol. 193, article 108406, 2022.

[7] R. Qian, M. Sellathurai, and D. Wilcox, "A study on MVDR beamforming applied to an ESPAR antenna," *IEEE Signal Processing Letters*, vol. 22, no. 1, pp. 67–70, 2015.

[8] R. O. Schmidt, "Multiple emitter location and signal parameter estimation," *IEEE Transactions on Antennas and Propagation*, vol. 34, no. 3, pp. 276–280, 1986.

[9] P. Stoica and A. Nehorai, "MUSIC, maximum likelihood, and Cramer-Rao bound," *IEEE Transactions on Acoustics Speech and Signal Processing*, vol. 37, no. 5, pp. 720–741, 1989.

[10] R. Roy and T. Kailath, "ESPRIT-estimation of signal parameters via rotational invariance techniques," *IEEE Transactions on Acoustics Speech and Signal Processing*, vol. 37, no. 7, pp. 984–995, 1989.

[11] H. Qiao and P. Pal, "On maximum-likelihood methods for localizing more sources than sensors," *IEEE Signal Processing Letters*, vol. 24, no. 5, pp. 703–706, 2017.

[12] P. Stoica and A. B. Gershman, "Maximum-likelihood DOA estimation by data-supported grid search," *IEEE Signal Processing Letters*, vol. 6, no. 10, pp. 273–275, 1999.

[13] M. Esfandiari, S. A. Vorobyov, S. Alibani, and M. Karimi, "Non-iterative subspace-based DOA estimation in the presence of nonuniform noise," *IEEE Signal Processing Letters*, vol. 26, no. 6, pp. 848–852, 2019.

[14] H. Zhou, G. Hu, J. Shi, and Z. Feng, "Novel diagonal reloading based direction of arrival estimation in unknown non-uniform noise," *Mathematical Problems in Engineering*, vol. 2018, Article ID 3084516, 9 pages, 2018.

[15] M. Agrawal and S. A. Prasad, "A modified likelihood function approach to DOA estimation in the presence of unknown spatially correlated Gaussian noise using a uniform linear array,"

IEEE Transactions on Signal Processing, vol. 48, no. 10, pp. 2743–2749, 2000.

[16] M. Guo, Y. Sun, J. Dai, and C. Chang, "Robust DOA estimation for burst impulsive noise," *Digital Signal Processing*, vol. 114, no. 4, article 103059, 2021.

[17] A. Paulraj and T. Kailatn, "Eigenstructure methods for direction of arrival estimation in the presence of unknown noise fields," *IEEE Transactions on Acoustics Speech and Signal Processing*, vol. 34, no. 1, pp. 13–20, 1986.

[18] M. Pesavento and A. B. Gershman, "Maximum-likelihood direction-of-arrival estimation in the presence of unknown nonuniform noise," *IEEE Transactions on Signal Processing*, vol. 49, no. 7, pp. 1310–1324, 2001.

[19] C. E. Chen, F. Lorenzelli, R. E. Hudson, and K. Yao, "Stochastic maximum-likelihood DOA estimation in the presence of unknown nonuniform noise," *IEEE Transactions on Signal Processing*, vol. 56, no. 7, pp. 3038–3044, 2008.

[20] Y. Wu, C. Hou, G. Liao, and Q. Guo, "Direction-of-arrival estimation in the presence of unknown nonuniform noise fields," *IEEE Journal of Oceanic Engineering*, vol. 31, no. 2, pp. 504–510, 2006.

[21] B. Liao, H. Lei, C. Guo, and H. C. So, "New approaches to direction-of-arrival estimation with sensor arrays in unknown nonuniform noise," *IEEE Sensors Journal*, vol. 16, no. 24, pp. 8982–8989, 2016.

[22] M. Wagner, Y. Park, and P. Gerstoft, "Gridless DOA estimation and root-music for non-uniform linear arrays," *IEEE Transactions on Signal Processing*, vol. 69, pp. 2144–2157, 2021.

[23] Q. Wu, F. Sun, P. Lan, G. Ding, and X. Zhang, "Two-dimensional direction-of-arrival estimation for co-prime planar arrays: a partial spectral search approach," *IEEE Sensors Journal*, vol. 16, no. 14, pp. 5660–5670, 2016.

[24] F. Yan, X. Li, T. Jin, L. Liu, and M. Jin, "A real-valued polynomial rooting method for fast direction of arrival estimation with large uniform linear arrays," *IEEE Access*, vol. 7, pp. 122330–122341, 2019.